Original Article

Skeletal, soft tissue, and airway changes following the alternate maxillary expansions and constrictions protocol

Berza Sen Yilmaz[a]; Nazan Kucukkeles[b]

ABSTRACT

Objective: To evaluate the skeletal, soft tissue, and airway effects of the alternate maxillary expansions and constrictions (Alt-RAMEC) protocol in prepubertal patients.

Materials and Methods: The appliance containing a double-hinged expansion screw was applied to 20 patients with Class III skeletal malocclusion characterized by maxillary retrognathia. The mean age of the study group was 9 years and 8 months. The patients' parents were instructed to open the screw by 1 mm per day during the first week and to close it by 1 mm per day the week after. This alternate opening and closing was repeated for 9 consecutive weeks. Cone beam computed tomography records and three-dimensional photographs were taken before treatment and after 9 week of the Alt-RAMEC protocol.

Results: Point A moved slightly forward (0.89 mm) and downward (0.92 mm) ($P < .05$). The average amount of expansion achieved at the level of point A was 5.54 mm ($P < .05$). Besides the maxilla, the expansive forces also affected the nasal bone, the zygomaticomaxillary and zygomaticotemporal sutures ($P < .05$). The soft tissue nasal width increased significantly. The airway volume of the anterior nasal compartment and the nasal cavity also increased ($P < .05$).

Conclusions: Slight forward movement of point A occurred with the Alt-RAMEC protocol. The expansion affected not only the maxilla but also other structures of the face. Significant cutaneous changes occurred in the paranasal area. Some significant increase in the upper airway volume was obtained. (*Angle Orthod.* 2015;85:117–126.)

KEY WORDS: Alt-RAMEC; Double-hinged expansion screw; Class III malocclusion; Airway

INTRODUCTION

Class III skeletal malocclusion is among the most challenging problems to treat in orthodontics. Maxillary retrognathia is an important component of Class III malocclusion. For adults, camouflage or surgical interventions are treatment options, whereas for younger patients maxillary retrognathia can be successfully corrected with early treatment. Rapid maxillary expansion (RME) combined with face mask therapy is a routine clinical procedure as it is assumed that RME disarticulates the circummaxillary sutures.[1–3] Liou[4] introduced a different method called "alternate rapid maxillary expansions and constrictions" (Alt-RAMEC). This protocol is performed with a special double-hinged expansion screw that is alternately opened and closed for 7 to 9 consecutive weeks.[4–6] Liou[7] stated that this special screw has an advantage in that the center of rotation can be located near the maxillary tuberosity, thereby enhancing the forward movement of maxilla. Liou and Tsai[5] reported a 3-mm advancement of point A with the Alt-RAMEC protocol and 5.8 mm of total advancement after protraction. This result is dramatic, as conventional RME+protraction procedures achieve an average advancement of only 1.5–3 mm.[8,9]

In the literature some articles report successful clinical results with this protocol, but because the second records are taken after protraction, the amount of advancement related solely to Alt-RAMEC protocol cannot be isolated.[10,11] Other than Liou and Tsai's study,[5] no other study has evaluated the pure effects of the Alt-RAMEC protocol.

In this study, we decided to test whether the Alt-RAMEC protocol can be an alternative treatment

[a] Clinical Instructor, Department of Orthodontics, Faculty of Dentistry, Bezmialem Vakif University, Istanbul, Turkey.

[b] Professor, Department of Orthodontics, Faculty of Dentistry, Marmara University, Istanbul, Turkey.

Corresponding author: Dr Berza Sen Yilmaz, Bezmialem Vakif Universitesi, Di[o] Hekimligi Fakültesi, Ortodonti Anabilim Dal[1], Vatan Caddesi 34093 Fatih, Istanbul, Turkey
(e-mail: berzasen@hotmail.com)

Accepted: January 2014. Submitted: September 2013.
Published Online: March 12, 2014

Figure 1. Double-hinged expansion device.

modality for mild skeletal discrepancies in preadolescent patients using three-dimensional (3D) imaging.

MATERIALS AND METHODS

The study group comprised 10 girls (~9 years 2 months old) and 10 boys (~10 years 3 months old) with maxillary retrognathia. The mean age of the group was 9 years 8 months.

The screw (US Patent No 6334771B1) was positioned parallel to the midline and the arms were bent to the buccal side to form the hooks for face mask application after expansion (Figure 1).

The parents were instructed to open the screw by 1 mm per day during the first week (two turns in the morning and two turns in the evening) and to close it by 1 mm per day the following week. This alternating opening and closing was repeated for 9 consecutive weeks.

Cone beam computed tomography (CBCT) images were taken before and after 9 weeks with an Iluma Imtec Imaging machine (3M, Ardmore, OK, USA), while patients were sitting in an upright position (x-ray tube, 120kV; x-ray tube current, 1–4 mA; scanning time, 40 seconds maximum and 7.8 seconds minimum; field of view, 14.2 × 21.1 cm; voxel size, 0.0936 mm; grey scale, 14 bit). In addition, ear-to-ear 3D photographs were shot using the 3dMDface system (3dMD LLC, Atlanta, GA, USA). The data was analyzed using MIMICS version 14.0 (Materialize Interactive Medical Image Control Systems, Leuven, Belgium). The study was approved by the Bezmialem University Ethical Committee.

Skeletal Evaluation

After the DICOM (digital imaging and communications in medicine) data were uploaded to the software, a full-head mask was created by calibrating the bone tissue. The mask containing the nasomaxillary complex and the head bones was obtained by subtracting the mandibular and vertebral masks from the main mask.

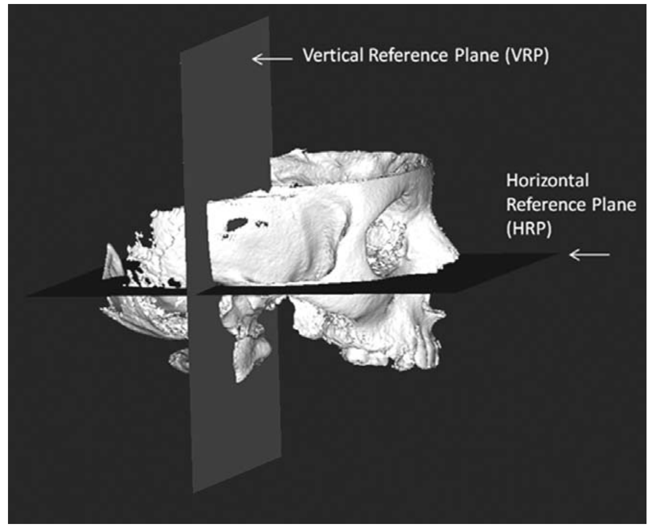

Figure 2. Vertical and horizontal reference planes.

Masks before and after the protocol were first superimposed, and the horizontal reference plane (HRP) was formed between the right and left porion and the right infraorbital point. The vertical reference plane (VRP) was formed by the plane passing through the porions, perpendicular to the HRP (Figure 2). The measurements were made to the same reference planes for the superimposed masks. Ten skeletal landmarks were defined and distances to HRP and VRP were measured together with five bilateral measurements (Figure 3a,b; Table 1).

Soft Tissue Evaluation

After cleaning all the artifacts, 3D photographs were superimposed using 3dMD patient software. The superimposed masks were transferred to MIMICS software in STL file format.

A vertical plane was created passing through the right and left inner cantus and the right alar curvature point. The junction point between the earlobe and the face skin was defined; a second plane parallel to the first plane passing through this point formed the soft tissue reference plane (STRP) (Figure 4).

The landmarks shown in Figure 5a,b and described in Table 1 (defined by Farkas[12]) were selected. The distances were measured from these points to STRP. The distances between right and left alar curvature (ac) and subalare (sbal) points were also registered.

Airway Evaluation

The airway mask was created by thresholding the DICOM data between −1024 and −400 HU. The plane passing through the right and left anterior clinoid processes and nasion formed the upper limit of the analyzed airway. The plane passing through the most

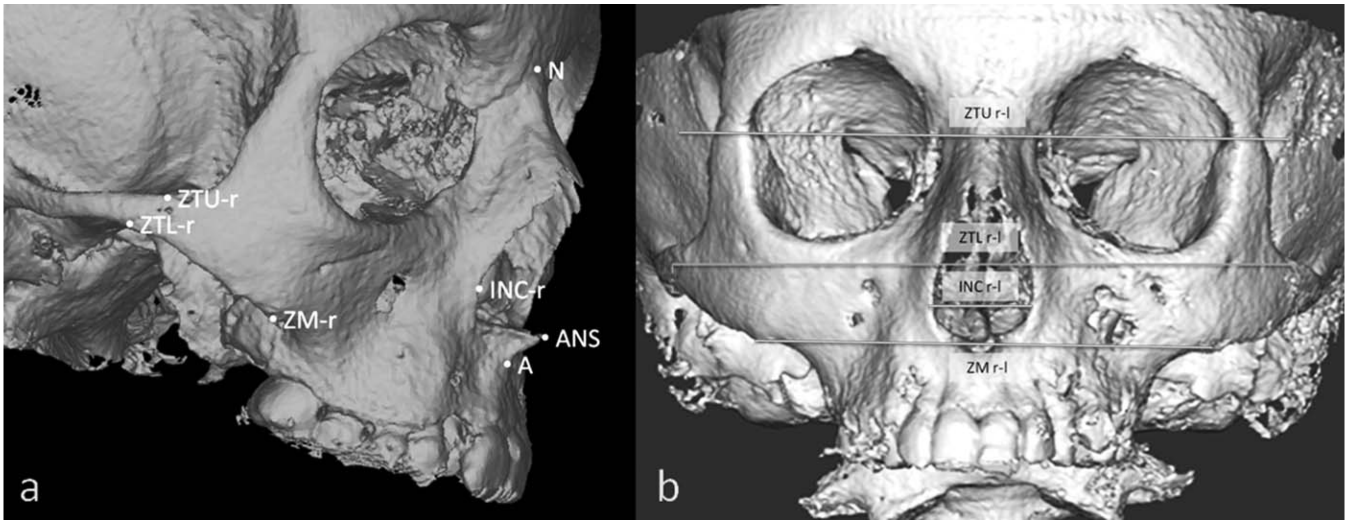

Figure 3. (a) Skeletal reference points. (b) Bilateral distance measurements.

anterior and the lowest bound of the second cervical vertebrae and parallel to the upper plane formed the lower limit. The outer air was separated with the plane passing through the nasal tip and the most convex points of the alar curvature.

The airway was divided into three parts; pharyngeal, nasal, and anterior nasal compartments (Figure 6). A plane was formed passing through the lowest and most anterior bound of the first vertebrae and parallel to the upper limit. This plane determined the upper limit of the

Table 1. Skeletal and Soft Tissue Landmarks and Measurements

Symbol	Name	Explanation
N	Nasion	Reference point corresponding to the middle point of the junction of the frontal and nasal bones
A	Point A	Point on the innermost curvature from the anterior nasal spine to the crest of the maxillary alveolar process
ANS	Anterior nasal spine	Pointed projection at the front extremity of the line of union of the two maxillae
INC	Inner nasal contour point	Bilateral landmark on the most curved anterior border of the aperture piriformis
ZM	Zygomaticomaxillary	Right and left lower borders of the zygomaticomaxillary suture
ZTU	Zygomaticotemporal upper	Right and left upper borders of the zygomaticotemporal suture
ZTL	Zygomaticotemporal lower	Right and left lower borders of the zygomaticotemporal suture
[A2 r-l]		Distance between the right and left A points created with the expansion forces
[INC r-l]		Distance between the right and left INC points
[ZTL r-l]		Distance between the right and left ZTL points
[ZTU r-l]		Distance between the right and left ZTU points
[ZM r-l]		Distance between the right and left ZM points
s	Sellion	Deepest midline point of the angle formed between the nose and forehead
en	Endocanthion	Bilateral landmark located at the medial corner of the eye where the upper and lower eyelids meet
ex	Exocanthion	Bilateral landmark located at the lateral corner of the eye where the upper and lower eyelids meet
prn	Pronasale	Most protrusive point on the nasal tip in the midline
ac	Alar curvature point	Bilateral landmark located where the nose wing ends and meets the skin of the cheek
sbal	Subalare	Bilateral landmark located below the nostril opening at the point where the semilunar continuation of the alar cartilage inserts into the skin of the upper lip
sb	Subnasale	Point located at the apex of the nasolabial angle in the midline, where the inferior border of the nasal septum meets the skin of the upper lip
c	Columella	Point located at the midline on the skinfold between the tip of the nose and the subnasale point at the level of the anterior border of the nostrils
ch	Chelion	Bilateral landmark located at the most lateral corner (commissure) of the mouth where the upper and lower lips meet
ls	Labiale superius	Midpoint of the upper vermilion line
chp	Christa philtri	Point on each elevated margin of the philtrum above the vermilion line
mlr	Malar point	Bilateral landmark equidistant between the chelion and the alar curvature point
inf	Infraorbital point	Bilateral landmark equidistant between the exocanthion and the alar curvature point
chk	Cheek point	Bilateral landmark equidistant between the exocanthion and the chelion
[sbal r-l]		Distance between the right and left subalare points
[ac r-l]		Distance between the right and left alar curvature points

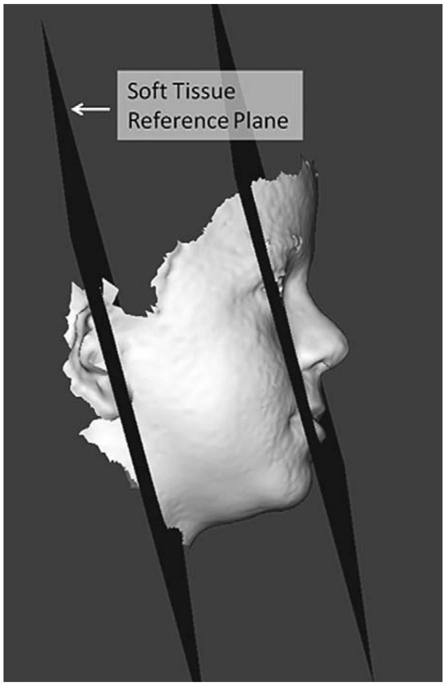

Figure 4. Soft tissue reference plane.

pharyngeal compartment. The nasal and anterior nasal compartments were separated with the plane passing through the sellion and bilateral ac points.

Statistical Analysis

Statistical Package for Social Sciences for Windows 15.0 software (SPSS Inc, Chicago, IL, USA) was used for the statistical analysis. The conformity of the parameters to the normal distribution was assessed by the Kolmogorov-Smirnov test and the

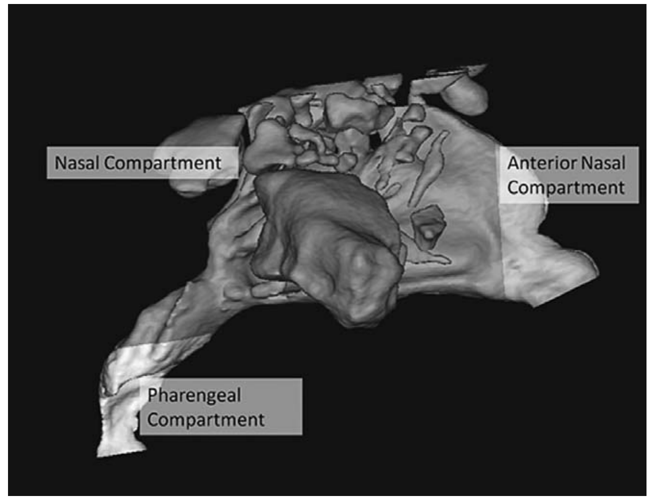

Figure 6. Three-dimensional mask of the airway divided into three compartments.

parameters conformed to the normal distribution. A paired samples *t*-test was used for in-group comparisons of the parameters. The intraclass correlation coefficient (ICC) was calculated for the analysis of the method error. Significance was evaluated at a level of $P < .05$.

RESULTS

All patients followed the protocol well, although a few patients reported discomfort over the nasal bone and the zygomatic ridges during constriction. Clinically, maxillary expansion and slight improvement of the overjet was recorded in all patients (Figures 7a,b, 8a through c, and 9a,b).

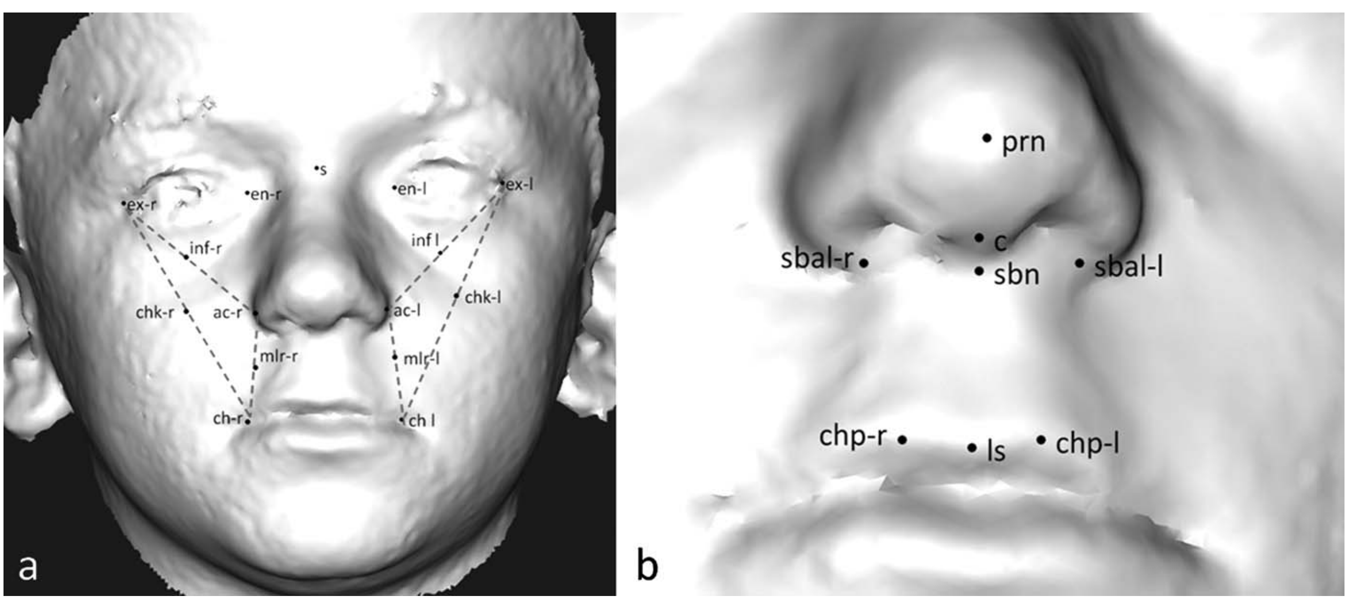

Figure 5. (a, b) Soft tissue reference points.

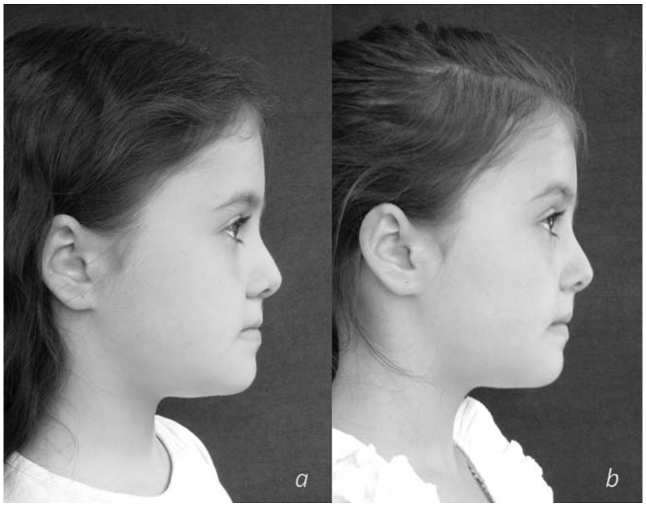

Figure 7. Extraoral photographs taken (a) before treatment and (b) after the Alt-RAMEC protocol.

The skeletal, soft tissue, and airway measurements were repeated by the same operator 3 weeks after the first measurement. Tables 2 through 4 present the ICC. The method is shown to be reliable and reproducible for all the analysis.

All the results presented in Tables 5 through 7 are mean change ± standard deviation. Point A moved slightly forward (0.89 ± 0.93 mm) and downward (0.92 ± 1.62 mm). The ANS moved slightly forward (0.76 ± 1.28 mm). The INC landmarks moved downward bilaterally (right, 0.83 ± 1.09 mm; left, 0.74 ± 1.24 mm). The INC-l point moved slightly upward (0.38 ± 0.78 mm) but no significant vertical change occurred for the right side. The ZTL right and left borders moved slightly upward (right, −0.31 ± 0.42 mm; left, −0.59 ± 0.57 mm) and the upper borders moved slightly downward (right, 0.26 ± 0.59 mm; left, 0.38 ± 0.45 mm). The right and left ZM landmarks moved backward (right, −0.60 ± 0.70 mm; left, −0.63 ± 0.79 mm). The amount of expansion achieved was 5.54 ± 1.48 mm at point A; 3.00 ± 1.4 mm at the nasal level; 1.61 ± 1.65 mm at the ZM level; and 0.75 ± 0.98 mm and 0.45 ± 0.82 mm at the ZTU and ZTL levels, respectively (Table 5).

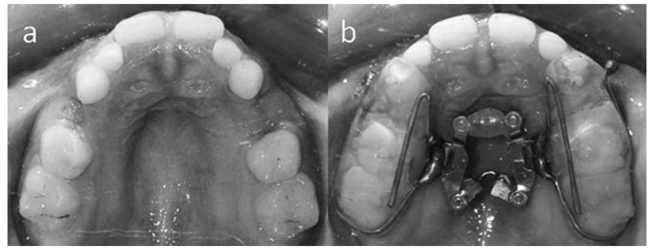

Figure 9. Intraoral occlusal view (a) before and (b) after the Alt-RAMEC protocol.

The distance between the ac points and the sbal points increased significantly (1.69 ± 1.08 mm and 1.16 ± 1.38 mm, respectively). The ac-r (1.20 ± 1.50 mm), sbal-r (0.71 ± 1.54 mm), and mlr-r (1.03 ± 1.78 mm) points moved forward. This forward movement also occurred for the left side, but the changes were not statistically significant (Table 6).

The volume of the anterior nasal compartment (376.42 ± 276.20 mm^3), volume of the nasal compartment (4632.28 ± 8165.95 mm^3), and total airway volume (5320.91 ± 8305.92 mm^3) increased significantly (Table 7).

DISCUSSION

The Alt-RAMEC duration varies from 4 to 9 weeks in different studies.[10,13] Liou[4,6,7] and Liou and Tsai[5] advise following the protocol for at least 7 weeks to obtain enough release of maxilla. We decided to follow the protocol for 9 weeks to ensure maxillary mobility and standardization of the method.

The 3D measurements have been shown to be more reliable than two-dimensional (2D) tracings.[14] The use of 3D imaging is crucial, especially for airway evaluation, because only surface measurements can be performed with 2D airway analysis.[15,16] Thus, we prefer to use 3D imaging systems to obtain more accurate data.

CBCT was selected instead of conventional computed tomography because the radiation dose is lower, the procedure is cheaper, and the image quality is still good.[17,18] According to the US Nuclear Regulatory

Figure 8. (a) Pretreatment intraoral view. (b) After bonding the device. (c) After the Alt-RAMEC protocol.

Table 2. Intraclass Correlation Coefficients (ICCs) of Skeletal Measurements[a]

		ICC	95% Confidence Interval
[A⊥VRP]	Before	0.995	0.982–0.999
	After	0.990	0.979–0.999
[A⊥HRP]	Before	0.968	0.876–0.992
	After	0.929	0.743–0.982
[A2 r-l]		0.920	0.712–0.979
[ANS⊥VRP]	Before	0.994	0.977–0.999
	After	0.995	0.981–0.999
[ANS⊥HRP]	Before	0.951	0.818–0.988
	After	0.983	0.933–0.996
[INC l⊥VRP]	Before	0.991	0.964–0.998
	After	0.970	0.886–0.993
[INC l⊥HRP]	Before	0.862	0.539–0.964
	After	0.895	0.636–0.973
[INC r⊥VRP]	Before	0.991	0.965–0.998
	After	0.983	0.933–0.996
[INC r⊥HRP]	Before	0.939	0.776–0.985
	After	0.963	0.860–0.991
[INC r-l-Sol]	Before	0.665	0.105–0.905
	After	0.863	0.544–0.964
[ZTL l⊥VRP]	Before	0.894	0.633–0.973
	After	0.843	0.488–0.958
[ZTL l⊥HRP]	Before	0.930	0.744–0.982
	After	0.928	0.739–0.982
[ZTL r⊥VRP]	Before	0.867	0.553–0.965
	After	0.733	0.234–0.926
[ZTL r⊥HRP]	Before	0.875	0.578–0.968
	After	0.857	0.526–0.962
[ZTL r-l]	Before	0.977	0.910–0.994
	After	0.977	0.911–0.994
[ZTU l⊥VRP]	Before	0.641	0.064–0.897
	After	0.677	0.127–0.909
[ZTU l⊥HRP]	Before	0.917	0.703–0.979
	After	0.870	0.562–0.966
[ZTU r⊥VRP]	Before	0.890	0.620–0.971
	After	0.831	0.458–0.955
[ZTU r⊥HRP]	Before	0.954	0.828–0.988
	After	0.905	0.666–0.976
[ZTU r-l]	Before	0.922	0.718–0.980
	After	0.937	0.768–0.984
[ZM l⊥VRP]	Before	0.969	0.881–0.992
	After	0.960	0.847–0.990
[ZM l⊥HRP]	Before	0.985	0.940–0.996
	After	0.983	0.933–0.996
[ZM r⊥VRP]	Before	0.948	0.806–0.987
	After	0.942	0.786–0.985
[ZM r⊥HRP]	Before	0.951	0.818–0.988
	After	0.974	0.897–0.993
[ZM r-l]	Before	0.909	0.679–0.977
	After	0.946	0.800–0.986

[a] HRP indicates horizontal reference plane; VRP, vertical reference plane; A, point A; ANS, anterior nasal spine; INC, inner nasal contour; ZTU-ZTL, upper and lower borders of the zygomaticotemporal suture; ZM, lower border of the zygomaticomaxillary suture; r, right; and l, left.

Table 3. Intraclass Correlation Coefficients (ICCs) of Soft Tissue Measurements[a]

		ICC	95% Confidence Interval
[s⊥STRP]	Before	0.933	0.500–0.993
	After	0.929	0.476–0.992
[sbal l⊥STRP]	Before	0.965	0.707–0.996
	After	0.958	0.661–0.996
[sbal r⊥STRP]	Before	0.954	0.630–0.995
	After	0.956	0.642–0.995
[ac l⊥STRP]	Before	0.954	0.632–0.995
	After	0.944	0.566–0.994
[ac r⊥STRP]	Before	0.951	0.614–0.995
	After	0.959	0.668–0.996
[sbal r-l]	Before	0.958	0.657–0.996
	After	0.989	0.899–0.999
[ac r-l]	Before	0.996	0.960–1.000
	After	0.993	0.935–0.999
[chk l⊥STRP]	Before	0.955	0.640–0.995
	After	0.943	0.560–0.994
[chk r⊥STRP]	Before	0.884	0.258–0.987
	After	0.868	0.290–0.985
[c⊥STRP]	Before	0.978	0.808–0.998
	After	0.958	0.657–0.996
[ls⊥STRP]	Before	0.943	0.558–0.994
	After	0.970	0.744–0.997
[inf l⊥STRP]	Before	0.942	0.555–0.994
	After	0.950	0.602–0.995
[inf r⊥STRP]	Before	0.903	0.343–0.989
	After	0.950	0.603–0.995
[chp l⊥STRP]	Before	0.962	0.687–0.996
	After	0.974	0.772–0.997
[chp r⊥STRP]	Before	0.957	0.649–0.995
	After	0.973	0.769–0.997
[mlr l⊥STRP]	Before	0.945	0.571–0.994
	After	0.966	0.712–0.996
[mlr r⊥STRP]	Before	0.925	0.457–0.992
	After	0.954	0.632–0.995
[prn⊥STRP]	Before	0.972	0.762–0.997
	After	0.967	0.722–0.997
[sb⊥STRP]	Before	0.971	0.754–0.997
	After	0.977	0.800–0.998

[a] STRP indicates soft tissue reference plane; s, sellion; ac, alar curvature point; sbal, subalare; prn, pronasale; c, columella; sb, subnasale; ls, labiale superius; chp, christa philtri; chk, cheek point; inf, infraorbital point; mlr, malar point; r, right; and l, left.

Commission, the amount of annual artificial radiation dose exposure limit is 1 mSv (Code of Federal Regulations, Title 10, §20.1301, Subpart D). The radiation dose of one CBCT scan is 0.058 mSv. Because we take two records in approximately 3 months, the dose exposure is still far below the annual limit (0.116 mSv).

In the literature little data have been published related to the pure effects of the Alt-RAMEC protocol. Thus, we have to compare our results with studies evaluating the conventional RME. We found that the maxilla moved slightly forward (0.8 mm) and downward (0.92 mm). Liou and Tsai[5] reported that the maxilla moved forward (3 mm) following the Alt-RAMEC protocol. The smaller amount of movement in our study might be explained by the skeletal differences in the cleft patients and the smaller sample size in their study. Moreover, it has been shown that measurements performed with 3D tomog-

Table 4. Intraclass Correlation Coefficients (ICCs) of Airway Measurements

		ICC	95% Confidence Interval
Pharyngeal compartment	Before	0.997	0.990–0.999
	After	0.996	0.983–0.999
Anterior nasal compartment	Before	0.981	0.925–0.995
	After	0.977	0.910–0.994
Nasal compartment	Before	0.999	0.995–1.000
	After	0.998	0.990–0.999
Total airway	Before	0.998	0.994–1.000
	After	0.997	0.989–0.999

raphy are more reliable than tracings made on 2D cephalograms.[14]

Some studies evaluating the effects of the Alt-RAMEC protocol followed by face mask application reported 2–5 mm forward movement of point A.[10,11] However, in such studies the amount of forward movement related to the Alt-RAMEC protocol cannot be isolated as the cephalometric records were taken after protraction.

In studies published by Podesser et al.[19] and Ballanti et al.,[20] 1.4 mm and 1.2 mm of increase were reported for the nasal cavity width measured at the level of the first molars; Christie et al.[21] reported 2.73 mm of widening. In our study, the expansion related to the nose is 3 mm, which seems to be larger than those reported, probably because our measuring points were located in the anterior part of the maxilla, where the largest expansion occurs. Moreover, those studies were performed with a conventional screw, whereas our study was performed with a double-hinged screw, which might have a different effect.

Besides the expansion of the maxillary bones, small but significant increases were found between the right and left upper/lower zygomaticotemporal (0.45–0.65 mm) and zygomaticomaxillary (1.61mm) points (Figure 3b). In the literature, several studies have reported that the circummaxillary sutures were affected by the RME protocol.[22–24] In a study performed by Leonardi et al.,[25] it is found that the RME also increased the bilateral distances of the zygomaticotemporal, zygomaticomaxillary, and other neighboring sutures.

On the other hand, the zygomaticomaxillary point presented backward movement. The upper borders of the zygomaticotemporal suture moved slightly downward, while the lower borders moved slightly upward. We can explain this with the triangular pattern of lateral movement of bone compartments during expansion. In the finite element morphometry study by Jafari et al.,[22] they found that expansive forces are not restricted to

Table 5. Skeletal Measurements Before and After the Alt-RAMEC Protocol[a]

	Before	After	Difference		
	Mean ± SD	Mean ± SD	Mean ± SD	*t*	*P*
[A⊥VRP]	81.95 ± 4.04	82.84 ± 4.01	0.89 ± 0.93	4.290	.001**
[A⊥HRP]	24.28 ± 2.92	25.21 ± 2.85	0.92 ± 1.62	2.553	.019*
[A2 r-l]	0.00 ± 0.00	5.54 ± 1.48	5.54 ± 1.48	16.705	.001**
[ANS⊥VRP]	86.90 ± 5.18	87.66 ± 4.94	0.76 ± 1.28	2.638	.016*
[ANS⊥HRP]	18.52 ± 2.82	18.80 ± 2.80	0.28 ± 0.82	1.526	.143
[INC l⊥VRP]	78.82 ± 4.09	79.65 ± 3.91	0.83 ± 1.09	3.427	.003**
[INC l⊥HRP]	11.04 ± 2.52	11.41 ± 2.65	0.38 ± 0.78	2.182	.042*
[INC r⊥VRP]	79.07 ± 4.67	79.81 ± 4.43	0.74 ± 1.24	2.680	.015*
[INC r⊥HRP]	10.76 ± 2.58	11.03 ± 2.72	0.28 ± 1.04	1.186	.250
[INC r-l]	19.93 ± 1.49	22.93 ± 1.80	3.00 ± 1.40	9.557	.001**
[ZTL l⊥VRP]	37.36 ± 2.94	36.93 ± 2.81	−0.42 ± 0.97	−1.938	.068
[ZTL l⊥HRP]	4.93 ± 1.74	4.35 ± 1.84	−0.59 ± 0.57	−4.621	.001**
[ZTL r⊥VRP]	38.31 ± 3.07	37.93 ± 3.26	−0.38 ± 0.97	−1.753	.096
[ZTL r⊥HRP]	4.90 ± 2.14	4.59 ± 1.90	−0.31 ± 0.42	−3.319	.004**
[ZTL r-l]	108.54 ± 4.48	109.29 ± 4.63	0.75 ± 0.98	3.404	.003**
[ZTU l⊥VRP]	45.44 ± 4.27	45.57 ± 4.07	0.13 ± 0.98	0.621	.542
[ZTU l⊥HRP]	2.42 ± 1.51	2.79 ± 1.53	0.38 ± 0.45	3.735	.001**
[ZTU r⊥VRP]	46.85 ± 3.41	46.86 ± 3.18	0.01 ± 0.90	0.030	.977
[ZTU r⊥HRP]	2.50 ± 1.42	2.76 ± 1.63	0.26 ± 0.59	1.945	.067
[ZTU r-l]	105.37 ± 4.68	105.81 ± 4.55	0.45 ± 0.82	2.433	.025*
[ZM l⊥VRP]	57.97 ± 2.89	57.34 ± 3.06	−0.63 ± 0.79	−3.547	.002**
[ZM l⊥HRP]	16.85 ± 2.44	16.53 ± 2.61	−0.32 ± 0.70	−2.025	.057
[ZM r⊥VRP]	58.44 ± 3.41	57.83 ± 3.21	−0.60 ± 0.70	−3.843	.001**
[ZM r⊥HRP]	16.76 ± 2.47	16.53 ± 2.46	−0.23 ± 0.63	−1.645	.116
[ZM r-l]	80.53 ± 3.37	82.14 ± 3.45	1.61 ± 1.65	4.359	.001**

[a] HRP indicates horizontal reference plane; VRP, vertical reference plane; A, point A; ANS, anterior nasal spine; INC, inner nasal contour; ZTU-ZTL, upper and lower borders of the zygomaticotemporal suture; ZM, lower border of the zygomaticomaxillary suture; r, right; and l, left.

* $P < .05$; ** $P < 0.01$ paired sample *t*-test.

Table 6. Soft Tissue Measurements Before and After the Alt-RAMEC Protocol

	Before	After	Difference		
	Mean ± SD	Mean ± SD	Mean ± SD	t	P
[s⊥STRP]	88.10 ± 4.48	88.21 ± 0.53	0.11 ± 0.71	0.690	.498
[ac l⊥STRP]	74.81 ± 3.57	75.48 ± 4.15	0.67 ± 1.55	1.930	.069
[ac r⊥STRP]	74.39 ± 3.70	75.59 ± 3.96	1.20 ± 1.50	3.587	.002**
[ac r-l distance]	29.97 ± 2.33	31.67 ± 2.42	1.69 ± 1.08	7.040	.001**
[sbal l⊥STRP]	77.06 ± 3.99	77.43 ± 4.32	0.37 ± 1.43	1.168	.257
[sbal r⊥STRP]	76.98 ± 4.05	77.69 ± 4.38	0.71 ± 1.54	2.064	.049*
[sbal r-l distance]	20.89 ± 1.90	22.06 ± 2.02	1.16 ± 1.38	3.781	.001**
[prn⊥STRP]	96.09 ± 4.31	94.41 ± 4.69	0.31 ± 1.40	0.992	.334
[c⊥STRP]	89.64 ± 4.00	89.89 ± 4.40	0.26 ± 1.43	0.803	.432
[sb⊥STRP]	81.37 ± 3.92	81.62 ± 4.44	0.26 ± 1.64	0.699	.493
[ls⊥STRP]	79.00 ± 3.85	78.83 ± 4.36	−0.17 ± 2.05	−0.376	.711
[chp l⊥STRP]	78.99 ± 4.00	78.82 ± 4.46	−0.17 ± 3.01	−0.388	.703
[chp r⊥STRP]	78.63 ± 3.90	78.84 ± 4.37	0.21 ± 2.03	0.465	.647
[chk l⊥STRP]	71.54 ± 4.12	71.79 ± 4.08	0.25 ± 1.14	0.977	.341
[chk r⊥STRP]	71.18 ± 3.71	71.52 ± 3.76	0.35 ± 1.37	1.125	.275
[inf l⊥STRP]	71.48 ± 3.89	71.29 ± 4.09	−0.19 ± 0.98	−0.858	.402
[inf r⊥STRP]	71.05 ± 3.71	71.21 ± 4.01	0.16 ± 1.24	0.583	.567
[mlr l⊥STRP]	73.23 ± 3.59	73.76 ± 4.14	0.53 ± 1.71	1.372	.186
[mlr r⊥STRP]	72.74 ± 3.61	73.77 ± 4.04	1.03 ± 1.78	2.588	.018*

[a] STRP indicates soft tissue reference plane; s, sellion; ac. alar curvature point; sbal, subalare; prn, pronasale; c, columella; sb, subnasale; ls, labiale superius; chp, christa philtri; chk, cheek point; inf, infraorbital point; mlr, malar point; r, right; and l, left.

* $P < .05$; ** $P < 0.01$ paired sample t-test.

the intermaxillary suture alone but are also distributed to the circummaxillary sutures.[22] It is reported that the anterior part of the maxilla was displaced downward but the zygomatic bone moved upward. In the anteroposterior plane, the maxilla was slightly displaced forward but the zygomatic bone showed backward displacement (0.75 mm).

In terms of soft tissue changes, the only significant change was related to the nasal width. Berger et al.[26] also showed that there was significant and stable change only for nasal width after RME (mean = 2 mm). Similarly, Johnson et al.[27] reported 1.1 mm of significant and stable increase in nasal width after RME. Pangrazio-Kulbersh et al.[28] performed a study to evaluate changes after RME with bonded and banded expanders. They reported that both appliances increased the skeletal and soft tissue dimensions of the nasal cavity, which supports our results. Nada et al.[29] reported slight lip and cheek changes. We also recorded similar changes, but our findings were not statistically significant.

It is assumed that widening the nasal passages and the nasal cavity with RME will result in improved breathing.[30–33] Haralambidis et al.[34] evaluated airway volume changes after RME and reported an 11.3% increase for the anterior nasal compartment. Our value was 9.67% for the same anatomic area ($P < .05$), but we did not record any significant change for the pharyngeal airway. Zhao et al.[35] and Pangrazio-Kulbersh et al.[28] had similar findings concerning the posterior airway.

It is reported in the literature that there are changes in airway dimensions related to the respiration phase and the tongue position.[36,37] No attempt was made during CBCT acquisition for our subjects to control respiratory movements and tongue posture. This problem can be minimized by training patients before scanning in future studies.

Table 7. Airway Measurements Before and After the Alt-RAMEC Protocol

	Before	After	Difference		
	Mean ± SD (mm³)	Mean ± SD (mm³)	Mean ± SD (mm³)	t	P
Anterior nasal compartment	1693.97 ± 397.44	2070.39 ± 545.95	376.42 ± 276.20	6.095	.001**
Nasal compartment	47,808.85 ± 12,265.54	52,441.13 ± 10,262.73	4632.28 ± 8165.95	2.537	.020*
Pharyngeal compartment	3196.35 ± 967.12	3508.56 ± 888.28	312.21 ± 806.95	1.730	.100
Total airway	52,699.17 ± 12,607.10	58,020.08 ± 10,624.56	5320.91 ± 8305.92	2.865	.011*

* $P < .05$; ** $P < 0.01$ paired sample t-test.

CONCLUSIONS

- The protocol caused expansion in the maxilla of prepubertal patients and also affected the neighboring sutures.
- The maxilla moved slightly forward and downward, but such a small change may have limited clinical utility.
- The Alt-RAMEC protocol cannot be a treatment option alone without the use of a protraction modality for patients with retrognathic maxilla.
- The soft tissue nasal width, anterior nasal volume, and nasal airway volume increased.

ACKNOWLEDGMENT

This study was supported by Marmara University Scientific Research Projects Commission (Project number SAG-C-DRP-101012-0318).

REFERENCES

1. Cozzani G. Extraoral traction and class III treatment. *Am J Orthod*. 1981;80:638–650.
2. Haas AJ. The treatment of maxillary deficiency by opening the midpalatal suture. *Angle Orthod*. 1965;35:200–217.
3. McNamara JA Jr. An orthopedic approach to the treatment of Class III malocclusion in young patients. *J Clin Orthod*. 1987;21:598–608.
4. Liou EJ. Toothborne orthopedic maxillary protraction in Class III patients. *J Clin Orthod*. 2005;39:68–75.
5. Liou EJ, Tsai WC. A new protocol for maxillary protraction in cleft patients: repetitive weekly protocol of alternate rapid maxillary expansions and constrictions. *Cleft Palate Craniofac J*. 2005;42:121–127.
6. Liou EJ. Effective maxillary orthopedic protraction for growing Class III patients: a clinical application simulates distraction osteogenesis. *Prog Orthod*. 2005;6:154–171.
7. Liou E. Interview. *Rev Dent Press Ortodon Ortop Facial*. 2009;14:27–37.
8. Ngan P, Hägg U, Yiu C, Merwin D, Wei SH. Treatment response to maxillary expansion and protraction. *Eur J Orthod*. 1996;18:151–168.
9. Williams MD, Sarver DM, Sadowsky PL, Bradley E. Combined rapid maxillary expansion and protraction facemask in the treatment of Class III malocclusions in growing children: a prospective long-term study. *Semin Orthod*. 1997;3:265–274.
10. Isci D, Turk T, Elekdag-Turk S. Activation-deactivation rapid palatal expansion and reverse headgear in Class III cases. *Eur J Orthod*. 2010;32:706–715.
11. Kaya D, Kocadereli I, Kan B, Tasar F. Effects of facemask treatment anchored with miniplates after alternate rapid maxillary expansions and constrictions: a pilot study. *Angle Orthod*. 2011;81:639–646. Epub Feb 7, 2011.
12. Farkas LG. *Anthropometry of the Head and Face in Medicine*. New York, NY: Elsevier Science Ltd; 1981.
13. Yen SL. Protocols for late maxillary protraction in cleft lip and palate patients at Childrens Hospital Los Angeles. *Semin Orthod*. 2011;17:138–148.
14. Varghese S, Kailasam V, Padmanabhan S, Vikraman B, Chithranjan A. Evaluation of the accuracy of linear measurements on spiral computed tomography-derived three-dimensional images and its comparison with digital cephalometric radiography. *Dentomaxillofac Radiol*. 2010;39:216–223.
15. Panou E, Motro M, Ateş M, Acar A, Erverdi N. Dimensional changes of maxillary sinuses and pharyngeal airway in Class III patients undergoing bimaxillary orthognathic surgery. *Angle Orthod*. 2013;83:824–831.
16. Kochel J, Meyer-Marcotty P, Sickel F, Lindorf H, Stellzig-Eisenhauer A. Short-term pharyngeal airway changes after mandibular advancement surgery in adult Class II-patients—a three-dimensional retrospective study. *J Orofac Orthop*. 2013;74:137–152.
17. Mah JK, Danforth RA, Bumann A, Hatcher D. Radiation absorbed in maxillofacial imaging with a new dental computed tomography device. *Oral Surg Oral Med Oral Pathol Oral Radiol Endod*. 2003;96:508–513.
18. Tsiklakis K, Donta C, Gavala S, Karayianni K, Kamenopoulou V, Hourdakis CJ. Dose reduction in maxillofacial imaging using low dose cone beam CT. *Eur J Radiol*. 2005;56:413–117.
19. Podesser B, Williams S, Crismani AG, Bantleon HP. Evaluation of the effects of rapid maxillary expansion in growing children using computer tomography scanning: a pilot study. *Eur J Orthod*. 2007;29:37–44.
20. Ballanti F, Lione R, Baccetti T, Franchi L, Cozza P. Treatment and posttreatment skeletal effects of rapid maxillary expansion investigated with low-dose computed tomography in growing subjects. *Am J Orthod Dentofacial Orthop*. 2010;138:311–317.
21. Christie KF, Boucher N, Chung CH. Effects of bonded rapid palatal expansion on the transverse dimensions of the maxilla: a cone-beam computed tomography study. *Am J Orthod Dentofacial Orthop*. 2010;137(suppl):S79–S85.
22. Jafari A, Shetty KS, Kumar M. Study of stress distribution and displacement of various craniofacial structures following application of transverse orthopedic force—a three-dimensional FEM study. *Angle Orthod*. 2003;73:12–20.
23. Yu HS, Baik HS, Sung SJ, Kim KD, Cho YS. Three-dimensional finite-element analysis of maxillary protraction with and without rapid palatal expansion. *Eur J Orthod*. 2007;29:118–125.
24. Starnbach H, Bayne D, Cleall J, Subtelny JD. Facioskeletal and dental changes resulting from rapid maxillary expansion. *Angle Orthod*. 1966;36:152–164.
25. Leonardi R, Sicurezza E, Cutrera A, Barbato E. Early post-treatment changes of circumaxillary sutures in young patients treated with rapid maxillary expansion. *Angle Orthod*. 2011;81:36–41.
26. Berger JL, Pangrazio-Kulbersh V, Thomas BW, Kaczynski R. Photographic analysis of facial changes associated with maxillary expansion. *Am J Orthod Dentofacial Orthop*. 1999;116:563–571.
27. Johnson BM, McNamara JA, Bandeen RL, Baccetti T. Changes in soft tissue nasal widths associated with rapid maxillary expansion in prepubertal and postpubertal subjects. *Angle Orthod*. 2010;80:995–1001.
28. Pangrazio-Kulbersh V, Wine P, Haughey M, Pajtas B, Kaczynski R. Cone beam computed tomography evaluation of changes in the naso-maxillary complex associated with two types of maxillary expanders. *Angle Orthod*. 2012;82:448–457.
29. Nada RM, van Loon B, Maal TJ, et al. Three-dimensional evaluation of soft tissue changes in the orofacial region after tooth-borne and bone-borne surgically assisted rapid maxillary expansion. *Clin Oral Investig*. 2013;Dec;17(9):2017–2024.

30. Hershey HG, Stewart BL, Warren DW. Changes in nasal airway resistance associated with rapid maxillary expansion. *Am J Orthod*. 1976;69:274–284.
31. Basciftci FA, Mutlu N, Karaman AI, Malkoc S, Küçükkolbasi H. Does the timing and method of rapid maxillary expansion have an effect on the changes in nasal dimensions? *Angle Orthod*. 2002;72:118–123.
32. Ramires T, Maia RA, Barone JR. Nasal cavity changes and the respiratory standard after maxillary expansion. *Braz J Otorhinolaryngol*. 2008;74:763–769.
33. Baratieri C, Alves M Jr, de Souza MM, de Souza Araújo MT, Maia LC. Does rapid maxillary expansion have long-term effects on airway dimensions and breathing? *Am J Orthod Dentofacial Orthop*. 2011;140:146–156.
34. Haralambidis A, Ari-Demirkaya A, Acar A, Küçükkeleş N, Ateş M, Ozkaya S. Morphologic changes of the nasal cavity induced by rapid maxillary expansion: a study on 3-dimensional computed tomography models. *Am J Orthod Dentofacial Orthop*. 2009;136:815–821.
35. Zhao Y, Nguyen M, Gohl E, Mah JK, Sameshima G, Enciso R. Oropharyngeal airway changes after rapid palatal expansion evaluated with cone-beam computed tomography. *Am J Orthod Dentofacial Orthop*. 2010;137(suppl):S71–S78.
36. Fregosi RF. Influence of tongue muscle contraction and transmural pressure on nasopharyngeal geometry in the rat. *J Appl Physiol*. 2011;111:766–774.
37. Grauer D, Cevidanes LS, Styner MA, Ackerman JL, Proffit WR. Pharyngeal airway volume and shape from cone-beam computed tomography: relationship to facial morphology. *Am J Orthod Dentofacial Orthop*. 2009;136:805–814.